RSC Advances




ROYAL SOCIETY OF CHEMISTRY

www.rsc.org/advances

Journal Name

ARTICLE

# Noble Gas Supported $B_3^+$ Cluster: Formation of Strong Covalent Noble Gas-Boron Bonds

Received 00th January 20xx,
Accepted 00th January 20xx

DOI: 10.1039/x0xx00000x
www.rsc.org/

Ranajit Saha,[1] Sudip Pan,[1] Subhajit Mandal,[1] Mesías Orozco,[2] Gabriel Merino*,[2] and Pratim K. Chattaraj*,[1]

The stability of noble gas (Ng) bound $B_3^+$ clusters is assessed via an *in silico* study, highlighting their structure and nature of the Ng-B bonds. Ar to Rn atoms are found to form exceptionally strong bonds with $B_3^+$ having each Ng-B bond dissociation energy in the range of 15.1-34.8 kcal/mol in $B_3Ng_3^+$ complexes with gradual increase in moving from Ar to Rn. The computed thermochemical parameters like enthalpy and free energy changes for the Ng dissociation processes from $B_3Ng_3^+$ also support the stability of Ar to Rn analogues for which the corresponding dissociation processes are endergonic in nature even at room temperature. The covalent nature of the Ng-B bonds is indicated by the localized natural Ng-B bond orbitals and high Wiberg bond indices (0.57-0.78) for Ng-B bonds. Electron density analysis also supports the covalency of these Ng-B bonds where the electron density gets accumulated in between Ng and B centres. The orbital interaction energy is the main contributor (*ca.* 63.0-64.4%) of the total attraction energy in Ng-B bonds. Furthermore, the Ng-B bonding can be explained in terms of a donor-acceptor model where the Ng (HOMO) → $B_3Ng_2^+$ (LUMO) σ-donation has the major contribution.

## Introduction

The first member of group 13, boron (B), has received much attention from the inorganic chemists[1] as well as from the theoreticians.[2] Boron being an electron deficient element shows interesting unusual chemical bonding patterns in boron clusters. In recent years, one-, two-centre as well as multi-centre boron species were experimentally synthesized which were found to be stabilized by σ-donor and π-acceptor ligands[3] exhibiting bizarre chemical bonding pattern. The tricoordinated borylene complexes were synthesized and generally designated using the formula: L → B(R) ← L,[1a,4] where L = N-heterocyclic carbenes (NHC), cyclic alkyl amino carbenes (CAAC), carbon monoxide (CO); R = H or bulky aryl group. Here, the single boron atom acts as a Lewis base. Diatomic $B_2$ having B≡B triple bond was also stabilized and isolated in L → B≡B ← L[5] (L = NHC, CAAC, CO, $BO^-$). All of the mentioned ligands are of σ-donor and π-acceptor type in nature. The B≡B triple bond length is correlated with the π-acceptor strength of L. Next discussion comes with triangular boron clusters. Theoretical calculations show that $B_3^+$ is the smallest π-aromatic[2a,6] system where the highest occupied molecular orbital (HOMO) is delocalized over the three B atoms. Recently, theoretically[7] NHC stabilized triangular $B_3^+$ cluster is predicted by Tai *et al*. but its experimental verification is still awaited. However, $[Ga_3R_3][M_2]$[8] and $[Al_3R_3][M_2]$[9] (M = Na, K; R = bulky aryl group) have been synthesized and isolated. Very recently, Frenking and co-workers[10] showed the formation of boron-carbonyl ($B_3(CO)_3^+$) and boron-dinitrogen ($B_3(NN)_3^+$) cations by using a pulsed laser and detected it in mass spectra. In those works, the bonding analyses showed that these $B_3L_3^+$ complexes are stabilized predominantly by L → $B_3L_2^+$ σ-donation.

The long controversy about the capability of noble gas (Ng) to form chemical bonds with other elements was ended in 1962 when Neil Bartlett reported the synthesis of xenon hexafluoroplatinate, $Xe^+(PtF_6)^-$.[11] In a very short interval, scientists reported the syntheses of $XeF_2$,[12] $XeF_4$,[13] $RnF_2$,[14] and $KrF_2$.[15] These pioneering works opened a new window for the search of new Ng compounds. In the last two decades, while a huge contribution to this field was made by the experimentalists[16] through the syntheses of different Ng compounds, the new prediction of Ng compounds along with the nature of bonding analyses in those synthesized and predicted compounds were also made by theoreticians.[17]

In general, there are two types of Ng compounds, first one being Ng insertion compounds within X-Y bond (XNgY) where X and Y cover a large range including H,[18a,18b,18c] F,[18b,18d,18e] Cl,[18c] Br,[18c] I,[18c], CN,[18c] $BN^-$,[18d] BN-R (R = H, CH3, CCH, CHCH2, F, and OH),[18e] BO,[18f] BS,[18g] $CO^+$,[18h] $CS^+$,[18i] $OSi^+$,[18j] CCH[18k] etc. and the second one being donor-acceptor type of compounds (NgXY) such as, NgLiX (X = H, F),[17j] NgBeX (X = O, S, $CO_3$, $SO_4$, NBO, NCN),[17d,17h,17v] and NgMX (M = Cu, Ag, Au; X = F, Cl, Br, CN, O),[16n-16s,17p,17w] where the Ng atom acts as an electron donor. Although a few number of Ng insertion compounds with Ng-B chemical bonds were reported in the literature, the number of examples of the latter type is rather scanty. First Ng inserted boron compound, $FXeBF_2$ was reported by Goetschel and Loos in 1979.[18l] Hu's group predicted a series of Ng inserted boron compounds such as FNgBO (Ng = Ar, Kr, Xe)[18f] and FNgBNR (Ng = Ar, Kr, Xe; R = H, $CH_3$, CCH, $CHCH_2$, F, OH).[18e] The stability of anionic $FNgBN^-$ (Ng = He-Rn) compounds,[18d] which are isoelectronic with FNgBO,[18f] was analyzed by Grandinetti and coworkers. Very recently, the stability of FNgBS[18g] and $HNgCS^+$[18i] was also investigated by Ghanty and coworkers. In these Ng

[1]Department of Chemistry and Centre for Theoretical Studies, Indian Institute of Technology Kharagpur, Kharagpur, 721302, India
[2]Departamento de Física Aplicada, Centro de Investigación y de Estudios Avanzados Unidad Mérida. km 6 Antigua Carretera a Progreso. Apdo. Postal 73, Cordemex, 97310, Mérida, Yuc., México
* Corresponding authors: gmerino@cinvestav.mx (GM), pkc@chem.iitkgp.ernet.in (PKC)

Electronic Supplementary Information (ESI) available: [details of any supplementary information available should be included here]. See DOI: 10.1039/x0xx00000x

inserted boron compounds, the bonds between B and Ng atoms are of covalent type as confirmed by different quantum chemical calculations. On the other hand, there are only two types of reported NgB species which have the donor-acceptor type of bonding. While the potential energy surfaces of $BNg^+$ (Ng = He, Ne and Ar)[18m] species are explored in 1971, Cooks and coworkers detected $BNg^+$ (Ng = Ar, Kr and Xe)[18n] in mass spectrometer by halogen/Ng exchange reaction in 1999. Ng supported boron-boron triple bond in Ng-B≡B-Ng (Ng = Ar, Kr) was also studied computationally and it shows remarkably strong Ng-B bonds.[18o]

Recently inert $N_2$ gas is stabilized with elongated N-N bond length in $B_3(NN)_3^+$.[10] This result shows $B_3^+$ is capable to bond with inert system. So it will be worth checking the binding ability of this $B_3^+$ cluster with inert gases and analyze the bonding nature in these complexes. In this work, we have reported the high stability of $B_3Ng_3^+$ clusters (Ng = Ar-Rn), thereby exploring the possibility of $B_3^+$ detection in Ng matrices. The dissociation energy, changes in enthalpy (ΔH) and Gibbs' free energy (ΔG) for the dissociation processes are computed to check the efficacy of the Ng binding ability of $B_3^+$ cluster. The nature of Ng-B bonding is analyzed through the natural bond orbital (NBO), electron density and energy decomposition (EDA) analyses. NBO analysis shows the presence of localized bond orbital in Ng-B bond, whereas the electron density analysis implies the Ng-B bonds to be of covalent type. Finally, EDA in conjunction with natural orbital for chemical valence (NOCV) indicates that the $B_3Ng_3^+$ complexes are mainly stabilized by Ng (HOMO) → $B_3Ng_2^+$ (LUMO) σ-donation.

## Computational Details

All the reported geometries of the studied $B_3Ng_3^+$ complexes are optimized using MP2[19] and CCSD(T)[20] methods along with Ahlrichs' basis sets, def2-TZVP and def2-QZVP.[21a] The effective core potential is used for the core electrons of Xe (ecp-28)[22] and Rn (ecp-46).[22] The harmonic vibrational frequency calculations are also done at the MP2/def2-TZVP level to find the nature of the stationary point and to compute the zero point energy (ZPE) correction and the thermochemical parameters. Due to expensive numerical frequency calculation at the CCSD(T)/def2-TZVP level, we have computed the frequency of the $B_3Ar_3^+$ complex only to check that the minimum energy structure is not an artifact of the MP2 level of computation. The absence of any imaginary frequency reveals that the studied complexes are minima on the corresponding potential energy surfaces. Here the ZPE corrected dissociation energy ($D_0$) values are provided. The dissociation of $B_3Ng_3^+$ is considered in two ways. In one way, $B_3Ng_3^+$ dissociates into $B_3^+$ and 3Ng atoms, thus $D_0$ is computed as,

$$D_0 = E_0(B_3^+) + 3E_0(Ng) - E_0(B_3Ng_3^+) \quad (1)$$

where $E_0$ are the ZPE corrected energies of $B_3^+$, Ngs and $B_3Ng_3^+$. Here, we have also computed the $D_0$ values at the complete basis set (CBS) limit. For this purpose, the energies obtained using the def2-TZVP and def2-QZVP basis sets are used and extrapolated them using the equation:

$$E(X) = E(\infty) + A\exp(-\alpha\sqrt{X}) \quad (2)$$

where E(X) and E(∞) are the energies obtained at X zeta basis sets (X = 3 for def2-TZVP and 4 for def2-QZVP) and at CBS limit, respectively. For def2 basis set with cardinal values 3 and 4, the α is found to be 7.88.[22b,22c]

In the second process, the successive dissociation is also considered via formation of $B_3Ng_2^+$, $B_3Ng^+$ and lastly $B_3^+$ where in each step one Ng atom gets detached. The optimization followed by frequency calculations are also done for $B_3Ng_2^+$ and $B_3Ng^+$ complexes at the MP2/def2-TZVP level. Natural population analysis (NPA)[24] and Wiberg bond index (WBI)[25] calculations are performed at the MP2/def2-TZVP level to compute the charge (q) at each atomic centre and the bond order, respectively, in NBO[26] scheme. All of the above calculations are carried out using the Gaussian 09 program package.[27]

The electron density descriptors at the bond critical point ($r_c$) of Ng-B bond are calculated by the topological analysis of the electron density[28] at the MP2/def2-TZVP/WTBS level using Multiwfn program.[29] The all electron WTBS basis set is used for Xe and Rn atoms.[30]

The EDA[31] is carried out in conjunction with NOCV at the revPBE-D3/TZ2P//MP2/def2-TZVP level using the ADF(2013.01) program package.[32] Grimme and coworkers[33] in their benchmark study have argued that the revPBE-D3 functional is one of the currently used most robust GGA functionals for related systems. Zeroth order regular approximation (ZORA)[34] is adopted to implement scalar relativistic effects for the heavier atoms like Xe and Rn. The EDA scheme decomposes the interaction energy ($\Delta E^{int}$) between the fragments into four contributing energy terms as,

$$\Delta E^{int} = \Delta E^{Pauli} + \Delta E^{elstat} + \Delta E^{orb} + \Delta E^{disp} \quad (3)$$

The repulsive Pauli interaction energy ($\Delta E^{Pauli}$) originated from the repulsion between the occupied orbitals at the interacting fragments. The term $\Delta E^{elstat}$ corresponds to the classical electrostatic energy between that fragments and it is generally attractive in nature. The next one is the attractive orbital interaction energy, $\Delta E^{orb}$, which arises from the charge transfer and mixing of the occupied and unoccupied orbitals on the fragments and polarization effect. The $\Delta E^{disp}$ takes care of the dispersion energy correction towards the interacting systems which is an important contribution for heavier elements. The sum of the three attractive energy factors predominates over the $\Delta E^{Pauli}$ and stabilizes the overall system. The EDA-NOCV[31,35] calculation further splits the total differential density Δρ(**r**) (corresponding to $\Delta E^{orb}$) into the deformation density ($\Delta\rho^i(\mathbf{r})$) and also shows the flow of the electron density. Each deformation density corresponds to the pair wise donation and back donation of electron density between those two fragments and $\Delta E_i^{orb}$ is the associated energy.

## Result and Discussion

### Geometries and Dissociation Energies

All the minimum energy structures of $B_3Ng_3^+$ are found to be at $D_{3h}$ point group symmetry and in $^1A'_1$ electronic state as depicted in Fig. 1. The results associated with the dissociation of $B_3Ng_3^+$ into $B_3^+$ and 3Ng atoms at the MP2/def2-TZVP, MP2/def2-QZVP, and MP2/CBS levels are provided in Table 1, whereas the same at the CCSD(T)/def2-TZVP level are presented in Table 1-SI. The ZPE corrected dissociation energy values ($D_0$) for the dissociation of $B_3Ng_3^+$ into $B_3^+$ and 3Ng atoms are in the range of 45.4-104.3

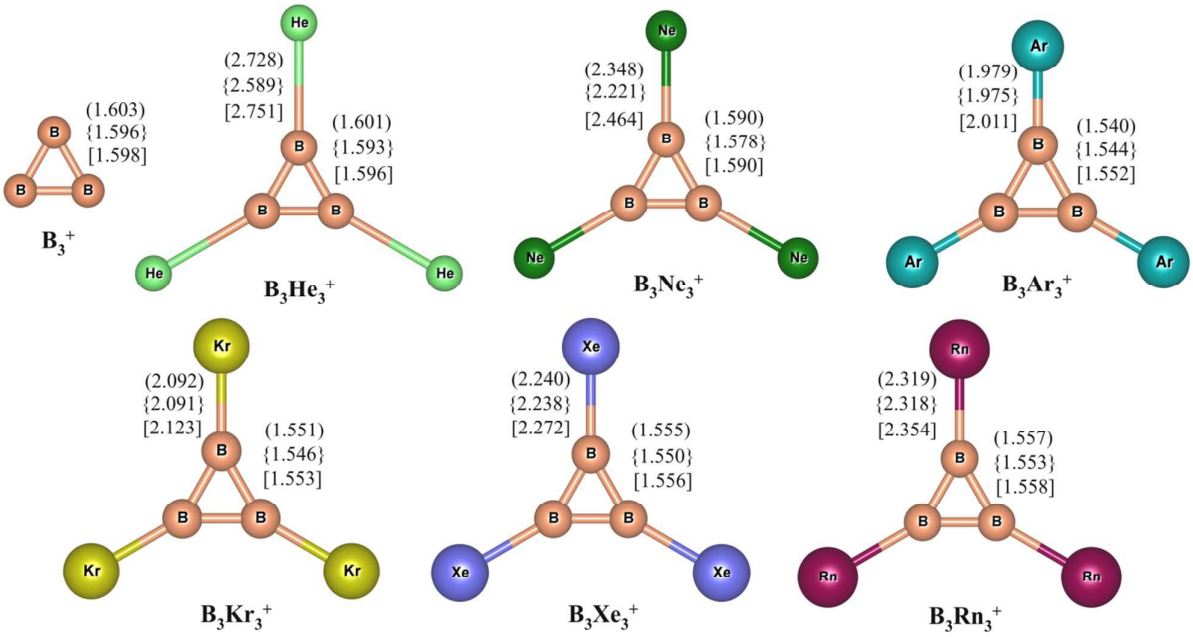


**Fig. 1.** Pictorial depiction of $B_3^+$ and $B_3Ng_3^+$ (Ng = He-Rn) complexes. All of the above structures are in $D_{3h}$ point group of symmetry and in $^1A_1'$ electronic state. The M-Ng bond distances are in Å unit and the values within first, second and square brackets are computed at the MP2/def2-TZVP, MP2/def2-QZVP and CCSD(T)/def2-TZVP level, respectively.

**Table 1.** ZPE corrected dissociation energy ($D_0$, kcal/mol) of Ng-B bonds, enthalpy change (ΔH, kcal/mol), and free energy change (ΔG, kcal/mol) at 298 K for the dissociation process: $B_3Ng_3^+ \rightarrow B_3Ng_2^+$ + 3Ng at the MP2/def2-TZVP, MP2/def2-QZVP and MP2/CBS levels.

| Complex | | $D_0$ | ΔH | ΔG |
|---|---|---|---|---|
| | MP2/def2-TZVP | 45.4 | 46.8 | 24.4 |
| $B_3Ar_3^+$ | MP2/def2-QZVP | 44.9 | 46.3 | 23.9 |
| | MP2/CBS | 44.9 | 46.3 | 23.8 |
| | MP2/def2-TZVP | 64.5 | 65.8 | 43.2 |
| $B_3Kr_3^+$ | MP2/def2-QZVP | 64.8 | 66.1 | 43.6 |
| | MP2/CBS | 64.8 | 66.1 | 43.6 |
| | MP2/def2-TZVP | 88.4 | 89.6 | 67.6 |
| $B_3Xe_3^+$ | MP2/def2-QZVP | 89.4 | 90.7 | 68.7 |
| | MP2/CBS | 89.6 | 90.8 | 68.8 |
| | MP2/def2-TZVP | 104.3 | 105.4 | 83.6 |
| $B_3Rn_3^+$ | MP2/def2-QZVP | 102.5 | 103.7 | 81.8 |
| | MP2/CBS | 102.3 | 103.4 | 81.5 |

kcal/mol for Ar-Rn analogues (or in the range of 15.1-34.8 kcal/mol for each Ng-B bond) at the MP2/def2-TZVP level, whereas $D_0$ values for the He and Ne analogues are very small as 0.4 and 3.4 kcal/mol, respectively (see Table 2-SI). As $D_0$ values are very small for He and Ne complexes, we have moved all the results associated with He and Ne to the supporting information (see Tables 2-SI - 6-SI and Fig. 1-SI and 2-SI). The results at the MP2/def2-QZVP level also show very similar $D_0$ values (difference ranging within 0.3-1.8 kcal/mol) with those at the MP2/def2-TZVP level. Further, the same values at the CBS limit are almost same as those obtained by the def2-QZVP basis set. Nevertheless, as the difference in $D_0$ values for each Ng-B bond is only 0.1-0.7 kcal/mol between def2-TZVP and CBS, we have continued with the def2-TZVP basis set.

On the other hand, $D_0$ values for each Ng-B bond are found to be overestimated at the MP2 level by an amount of 0.2-4.2 kcal/mol compared to the CCSD(T) level, except for the case of He (see Table 1-SI). The $D_0$ values at the CCSD(T) level are computed by using the ZPE correction obtained from the MP2 level. Only for $B_3Ar_3^+$, the ZPE correction obtained from the CCSD(T) level is included and the corresponding $D_0$ value is found to be 2.1 kcal/mol lower than that at the MP2 level. The corresponding Ng-B bond distance is also found to be longer by ~0.03 Å at the CCSD(T) level compared to the MP2 level. The increasing order of $D_0$ values from Ar to Rn analogues is obvious from its increase in the polarizability of the Ng atom along the group. The thermochemical parameters like ΔH and ΔG are also computed at 298 K and at one atmospheric pressure. The calculated ΔH values are found to be highly positive for all Ar-Rn analogues implying highly endothermic nature of the dissociation processes. The corresponding ΔG values reveal that the $B_3Ng_3^+$ complexes are stable enough at room temperature. Note that the dissociation of $B_3Ng_3^+$ into $B_3^+$ and 3Ng atoms is entropically favorable process, but the high positive ΔH predominates over the TΔS term, making the dissociation process non-spontaneous one.

The energy difference ($\Delta E_{H-L}$) between the HOMO and LUMO is a stability indicator of a system. The high value of $\Delta E_{H-L}$ means that the given system is reluctant either to add an electron in LUMO or to remove an electron from HOMO. The $\Delta E_{H-L}$ value for $B_3^+$ is found

**Table 2.** HOMO-LUMO energy gap ($\Delta E_{H-L}$, eV) , NPA charges on B and Ng centres (q, au), Wiberg bond indices of Ng-B and B-B bonds (WBI), Ng-B and B-B bond distances (r, Å) in $B_3Ng_3^+$ at the MP2/def2-TZVP level.

| $\Delta E_{H-L}$ | $q_B$ | $q_{Ng}$ | $WBI_{Ng-B}$ | $WBI_{B-B}$ | $r_{Ng-B}$ | $r_{B-B}$ | $r^{cov}_{B-Ng}$ [a] |
|---|---|---|---|---|---|---|---|
| 8.61 | 0.33 | | | 1.56 | | 1.603 | |
| 11.08 | -0.03 | 0.37 | 0.57 | 1.48 | 1.979 | 1.540 | 1.900 |
| 10.92 | -0.12 | 0.45 | 0.67 | 1.46 | 2.092 | 1.551 | 2.000 |
| 10.54 | -0.23 | 0.56 | 0.78 | 1.44 | 2.240 | 1.555 | 2.240 |
| 10.10 | -0.24 | 0.57 | 0.78 | 1.44 | 2.319 | 1.557 | 2.340 |

[a] $r^{cov}_{B-Ng}$ is calculated by taking summation of the covalent radii given in reference 36.

to be 8.61 eV (see Table 2), whereas the increased $\Delta E_{H-L}$ values are 11.08, 10.92, 10.54 and 10.10 eV for Ar, Kr, Xe and Rn bound analogues, respectively. Thus, upon binding with Ng atoms the system becomes more stable than the bare one.

**Successive Dissociation**

To get further insight into the stability of intermediate complexes, we have also computed $D_0$, ΔH and ΔG for the successive detachment of Ng atoms from $B_3Ng_3^+$ which leads to the formation of $B_3Ng_2^+$, $B_3Ng^+$ and at last the bare $B_3^+$ cluster (see Table 3 and Fig. 2). The related geometrical parameters are provided in Table 6-SI. The $D_0$, ΔH and ΔG values associated with the first, second and third dissociations of the Ng atoms are abbreviated as 1, 2 and 3 in their superscript, respectively. The $D_0$ value for the first dissociation is the lowest followed by the second dissociation then the third one, i.e., $D_0^1 < D_0^2 < D_0^3$. The thermochemical parameters also follow the same order. These results imply that the successive Ng binding ability drops significantly with the gradual increase in the number of Ng atoms. In fact, the strength of Ng-B bonds becomes almost half in additional Ng binding with $B_3Ng^+$. It may also be noted that the first Ar detachment process from $B_3Ar_3^+$ is exergonic by -0.6 kcal/mol at room temperature, which indicates that slightly lower temperature is needed to make $B_3Ar_3^+$ viable. The decrease in Ng-B bond strength gradually becomes larger in going from Ar to Rn. This is related to the degree of Ng → B electron donation populating the electron density within $B_3^+$ moiety. For first Ng, such electron donation is significantly high as it is shifted to a positively charged $B_3$ moiety. However, as a result of this electron donation the electropositive nature of $B_3$ diminishes and consequently for the second and third Ng atoms such donation gets increasingly more reduced, resulting in a lower Ng-B bond strength with an increase in the number of Ng atoms (see Table 3). Note that such Ng → B

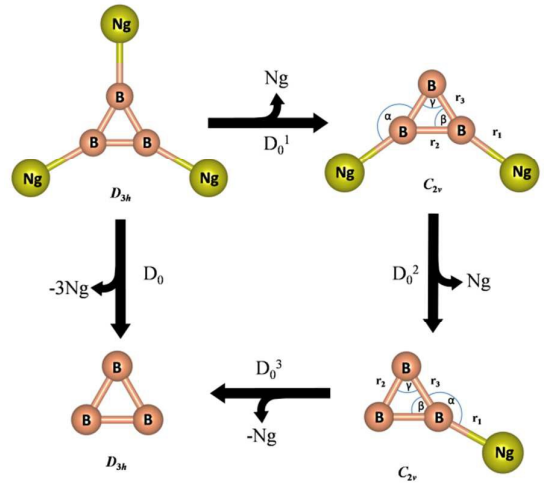


**Fig. 2.** The successive dissociation of Ng atom from $B_3Ng_3^+$ via $B_3Ng_2^+$, $B_3Ng^+$ and to the bare $B_3^+$ cluster.

electron donation is a major stabilizing factor for such complexes as obtained from the EDA (*vide infra*). Further, since the extent of Ng→B electron donation is increasing larger along Ar-Rn, such drop in $D_0$ value is more prominent along the same. With an increase in number of Ng atoms, the repulsion between two neighbouring Ng atoms would also contribute to some extent in reducing the Ng-B bond energy and it would be greater for the heavier Ng atoms.

**Mixed Complexes**

The possibility of mixed Ng bound $B_3^+$ cluster is studied by considering two types of Ng bound $B_3^+$ systems, $B_3XYZ^+$ an $B_3X_2Y^+$ (X, Y and Z are Ng atoms). In the first type, all the Ng atoms are different and in the second case one Ng atom differs from the others two. The corresponding results are provided in Table 4 and the related geometries are presented in Figs. 3 and 4. The results show that in the presence of heavier Ng atom in $B_3XYZ^+$ and $B_3X_2Y^+$, the $D_0$ value for the lighter Ng-B bonds decreases, whereas the heaviest Ng-B bond gets stronger. As for example, the $D_0$ value for Ar-B bond decreases to 3.2 kcal/mol in $B_3ArKrXe^+$, 2.6 kcal/mol in $B_3ArKrRn^+$,2.0 kcal/mol in $B_3ArXe_2^+$ and 4.4 kcal/mol in $B_3Ar_2Xe^+$ from 7.0 kcal/mol in $B_3Ar_3^+$. A similar result is also noted for Kr. But

**Table 3.** ZPE corrected successive dissociation energy ($D_0$, kcal/mol) of Ng-B bonds, enthalpy change (ΔH, kcal/mol) at 298 K, free energy change (ΔG, kcal/mol) for the respective dissociation process at 298 K, NPA charges on B and Ng centres (q, au), Wiberg bond indices of Ng-B (WBI) of their respective mother moiety at the MP2/def2-TZVP level.

| Ng | $B_3Ng_3^+$ [a] ⟶ $B_3Ng_2^+$ + Ng | | | $B_3Ng_2^+$ ⟶ $B_3Ng^+$ + Ng | | | | | | $B_3Ng^+$ ⟶ $B_3^+$ + Ng | | | | | |
|---|---|---|---|---|---|---|---|---|---|---|---|---|---|---|---|
| | $D_0^1$ | $\Delta H^1$ | $\Delta G^1$ | $D_0^2$ | $\Delta H^2$ | $\Delta G^2$ | $q_B$ [b] | $q_{Ng}$ | WBI | $D_0^3$ | $\Delta H^3$ | $\Delta G^3$ | $q_B$ [b] | $q_{Ng}$ | WBI |
| Ar | 7.0 | 7.2 | -0.6 | 14.0 | 14.5 | 6.9 | -0.09 | 0.42 | 0.64 | 24.4 | 25.1 | 18.0 | -0.18 | 0.47 | 0.71 |
| Kr | 10.7 | 10.9 | 3.0 | 20.0 | 20.4 | 12.9 | -0.19 | 0.52 | 0.75 | 33.8 | 34.5 | 27.4 | -0.30 | 0.58 | 0.82 |
| Xe | 15.3 | 15.5 | 8.0 | 27.2 | 27.6 | 20.1 | -0.30 | 0.64 | 0.86 | 45.9 | 46.5 | 39.5 | -0.43 | 0.72 | 0.93 |
| Rn | 19.1 | 19.3 | 11.8 | 32.0 | 32.4 | 24.9 | -0.31 | 0.66 | 0.87 | 53.2 | 53.8 | 46.9 | -0.44 | 0.75 | 0.95 |

[a] for the NPA charges on B and Ng centres (q, au), Wiberg bond indices of Ng-B (WBI) of $B_3Ng_3^+$ see Table 2; [b] $q_B$ is the charge of that boron atom which is bonded to Ng-atom; The superscript 1, 2 and 3 denote the first, second and third dissociation process.

**Table 4.** ZPE corrected dissociation energy ($D_0$, kcal/mol) of Ng-B bonds, enthalpy change (ΔH, kcal/mol), and free energy change (ΔG, kcal/mol) at 298 K for the dissociation process: $B_3XYZ^+ \rightarrow B_3XY^+ + Z$ (X, Y and Z = Ng, which includes Ar, Kr, Xe and Rn) at the MP2/def2-TZVP level.

| Dissociation Process | $D_0$ | ΔH | ΔG |
|---|---|---|---|
| $B_3ArKrXe^+ \longrightarrow B_3KrXe^+ + Ar$ | 3.2 | 3.4 | -3.6 |
| $B_3ArKrXe^+ \longrightarrow B_3ArXe^+ + Kr$ | 10.6 | 10.8 | 3.7 |
| $B_3ArKrXe^+ \longrightarrow B_3ArKr^+ + Xe$ | 20.6 | 20.7 | 13.7 |
| $B_3ArKrRn^+ \longrightarrow B_3KrRn^+ + Ar$ | 2.6 | 2.8 | -4.2 |
| $B_3ArKrRn^+ \longrightarrow B_3ArRn^+ + Kr$ | 9.9 | 10.1 | 3.1 |
| $B_3ArKrRn^+ \longrightarrow B_3ArKr^+ + Rn$ | 26.2 | 26.2 | 19.4 |
| $B_3ArXe_2^+ \longrightarrow B_3Xe_2^+ + Ar$ | 2.0 | 2.2 | -4.7 |
| $B_3ArXe_2^+ \longrightarrow B_3ArXe^+ + Xe$ | 18.9 | 19.0 | 11.8 |
| $B_3Ar_2Xe^+ \longrightarrow B_3ArXe^+ + Ar$ | 4.4 | 4.6 | -2.9 |
| $B_3Ar_2Xe^+ \longrightarrow B_3Ar_2^+ + Xe$ | 22.2 | 22.3 | 15.4 |
| $B_3Kr_2Xe^+ \longrightarrow B_3KrXe^+ + Kr$ | 9.1 | 9.3 | 1.6 |
| $B_3Kr_2Xe^+ \longrightarrow B_3Kr_2^+ + Xe$ | 18.9 | 19.0 | 11.9 |

the Xe-B bond in these mixed complexes (when Rn is not present) becomes stronger when compared with Xe-B bond in $B_3Xe_3^+$ complex. The $D_0$ value of Xe-B bond in $B_3Xe_3^+$ complex is 15.3 kcal/mol, which is enhanced by 5.3 kcal/mol in $B_3ArKrXe^+$, 3.6 kcal/mol in $B_3ArXe_2^+$ and 6.9 kcal/mol in $B_3Ar_2Xe^+$ complexes. Rn also follows the same trend as Xe, but the relative increase in Rn-B bond energy is higher than those in Xe analogues. Therefore, the present results show that if a mixture of Ngs remains present in the systems, only pure complexes of type $B_3X_3^+$ would be formed exclusively where the complexes with heaviest Ng atoms would be present in the largest proportion. Even if the complexes like $B_3XYZ^+$ and $B_3X_2Y^+$ are formed, they would be in very small proportion as the lighter Ng atoms would be spontaneously replaced by the heavier one.

**NBO Analysis**

The total charge on the bare $B_3^+$ system is equally divided among the three B atoms as 0.33 |*e*| on each B centre. Upon binding with Ng atoms, huge changes in the electronic charge distribution

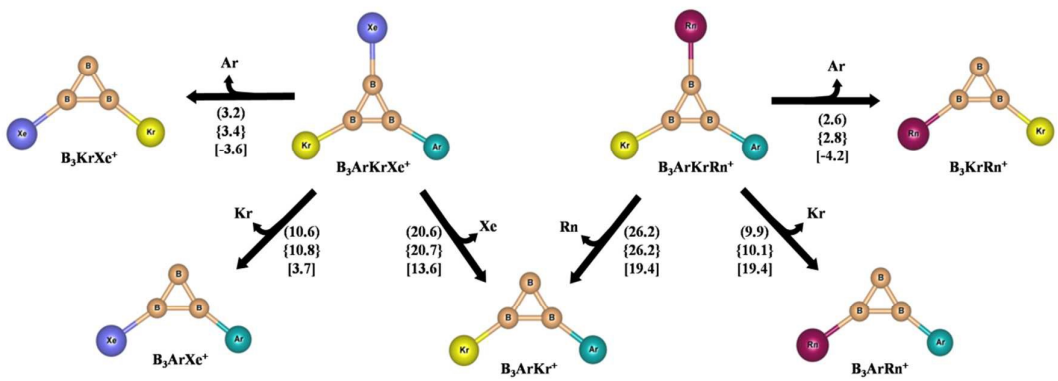


**Fig. 3.** The dissociation of different $B_3XYZ^+$ producing $B_3XY^+$ and Z (X, Y and Z are Ng atoms, which includes Ar, Kr, Xe and Rn). Values in first, second and third braces indicates $D_0$, ΔH and ΔG values respectively at the MP2/def2-TZVP level.

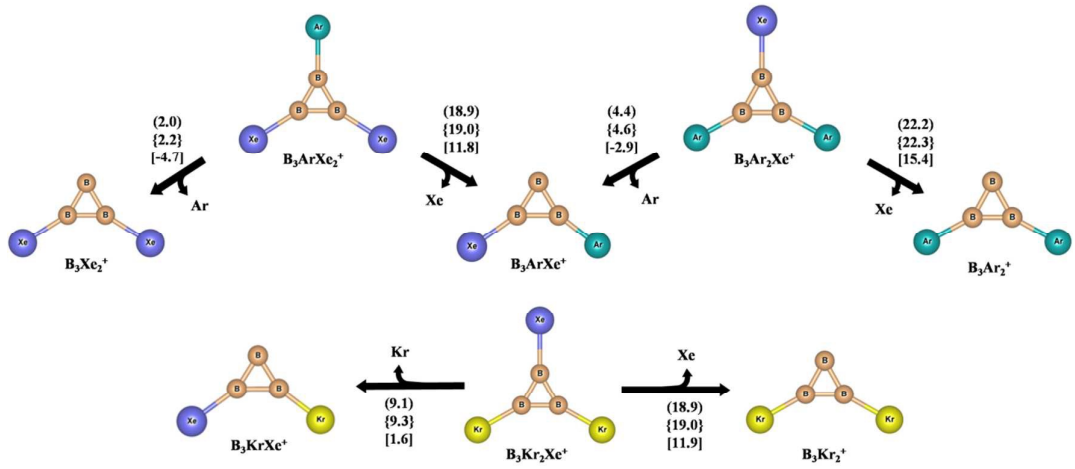


**Fig. 4.** The dissociation of different $B_3X_2Y^+$ producing $B_3X_2^+$ and Y or $B_3XY^+$ and X (X and Y are Ng atoms, which includes Ar, Kr, Xe). Values in first, second and third braces indicates $D_0$, ΔH and ΔG values respectively at the MP2/def2-TZVP level.

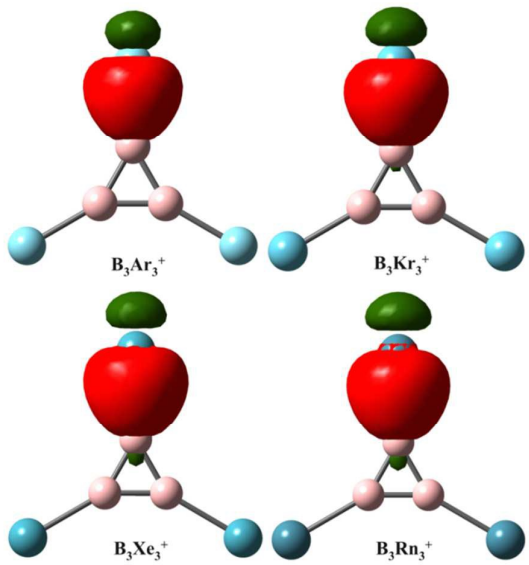


**Fig. 5.** The plot of natural bond orbitals (NBO) of Ng-B bonds in $B_3Ng_3^+$ (Ng = Ar – Rn) clusters.

occur (see Table 2). The Ng atoms acquire positive charges on it, whereas the B centres become negatively charged for the Ar to Rn analogous. From this result one can undoubtedly draw the picture of Ng → B charge transfer. The gradual increase in the charge transfer from Ar to Rn is described by the increase in the polarizability of the Ng centres. The WBI values range from 0.57 to 0.78 for Ar to Rn. The high WBI values indicate that there must be a covalent type of interaction in between the B and Ng atomss. The optimized Ar-B and Kr-B bond lengths are found to be closer to the sum of the corresponding covalent radii of the atoms while the Xe-B bond length is equal to the sum of their covalent radii and Rn-B bond length is shorter than the sum of their covalent radii.[36]Thus, there must be a covalent interaction between the Ng and B centres. Detailed NBO analysis shows the formation of three Ng-B bond orbitals which are equivalent due to symmetry for a given $B_3Ng_3^+$ complex as shown in Fig. 5. The occupancies of these NBOs are found to be close to 2.0, which again proves that the Ng-B is a covalent bond. The Ng-B NBOs are polarized with 72.5-82.4% towards the Ng atom (see Table 5) and p-orbitals take major part in the bonding with 72.0-82.9% from Ng side and 77.5-78.6% from B side.

**Electron Density Descriptors**

The Ng-B bond is further discussed in the light of electron density analysis proposed by Bader[28]. A covalent bond can be characterized in terms of the accumulation of the electron density ($\rho(r_c)$) in between the two atomic centres. The Laplacian of the electron density ($\nabla^2\rho(r_c)$) at $r_c$ is negative for a covalent bond i.e., $\nabla^2\rho(r_c)< 0$, whereas $\nabla^2\rho(r_c)> 0$ indicates charge depletion at $r_c$, hence a noncovalent bond. However, there are many examples like, systems

**Table 5.** The NBO occupancy (|*e*|), contribution from the atoms constructing that NBO and atomic contributions towards that NBO for $B_3Ng_3^+$ (Ng = Ar – Rn) complexes are presented at the MP2/def2-TZVP level.

| Complex | NBO | Occ. | Atomic Contribution | Atomic orbitals contribution to NBO | |
|---|---|---|---|---|---|
| | | | | Ng | B |
| $B_3Ar_3^+$ | B-Ar | 1.999 | B(17.6%)<br>Ar(82.4%) | s ( 27.8%)<br>p ( 72.0%) | s ( 20.5%)<br>p ( 78.6%) |
| $B_3Kr_3^+$ | B-Kr | 1.999 | B(21.7%)<br>Kr(78.3%) | s ( 24.1%)<br>p ( 75.8%) | s ( 21.2%)<br>p ( 77.9%) |
| $B_3Xe_3^+$ | B-Xe | 1.999 | B(26.9%)<br>Xe (73.1%) | s ( 21.0%)<br>p ( 78.8%) | s ( 21.7%)<br>p ( 77.3%) |
| $B_3Rn_3^+$ | B-Rn | 1.998 | B(27.5%)<br>Rn(72.5%) | s ( 17.0%)<br>p ( 82.9%) | s ( 21.7%)<br>p ( 77.5%) |

with heavier atom[37] and some covalent compounds like $F_2$[37d] and CO[28], where the criterion based on $\nabla^2\rho(r_c)$ fails to predict the covalent bond correctly. Cremer and Kraka[37d] suggested the use of local energy density, $H(r_c)< 0$ as another indicator to describe the covalency of a bond, where $H(r_c) = G(r_c) + V(r_c)$, and $G(r_c)$ and $V(r_c)$ are local kinetic energy density and local potential energy density, respectively. The $\nabla^2\rho(r_c)< 0$ is found for the Xe-B and Rn-B bonds whereas the Ar-B and Kr-B bonds have $\nabla^2\rho(r_c)> 0$, but $H(r_c)< 0$, indicating the covalency of these bonds (see Table 6). The contour plots of $\rho(r_c)$ and $\nabla^2\rho(\mathbf{r})$ for the $B_3Ng_3^+$complexes are depicted in Fig. 6 in which black solid lines shows the $\rho(r_c)$; blue solid lines show the region of $\nabla^2\rho(\mathbf{r})> 0$ and magenta dashed lines highlight the area of $\nabla^2\rho(\mathbf{r})< 0$ (see Fig. 1-SI for He and Ne). It is obvious from the contour plots of $\rho(r_c)$ that the electron density of Ngs becomes polarized towards B centres and the degree of deformation in electron density gradually increases in moving towards the heavier Ng atoms. The plots of $\nabla^2\rho(\mathbf{r})$ reveal that in all the cases, electron density is accumulated in between B and Ng centres and the region of such accumulation becomes gradually larger along Ar to Rn. In cases of Ar and Kr, the bond critical point lies slightly outside the region of electron density accumulation.

**Table 6.** Electron density descriptors (au) at the bond critical points ($r_c$) in between Ng and B atoms in $B_3Ng_3^+$ (Ng = Ar - Rn) obtained from the wave functions generated at the MP2/def2-TZVP/WTBS//MP2/def2-TZVP level. (All electron WTBS basis set is used only for Xe and Rn).

| Complex | $\rho(r_c)$ | $\nabla^2\rho(r_c)$ | $G(r_c)$ | $V\rho(r_c)$ | $H(r_c)$ |
|---|---|---|---|---|---|
| $B_3Ar_3^+$ | 0.066 | 0.157 | 0.086 | -0.132 | -0.046 |
| $B_3Kr_3^+$ | 0.071 | 0.056 | 0.071 | -0.127 | -0.057 |
| $B_3Xe_3^+$ | 0.080 | -0.062 | 0.055 | -0.125 | -0.070 |
| $B_3Rn_3^+$ | 0.082 | -0.124 | 0.032 | -0.095 | -0.063 |

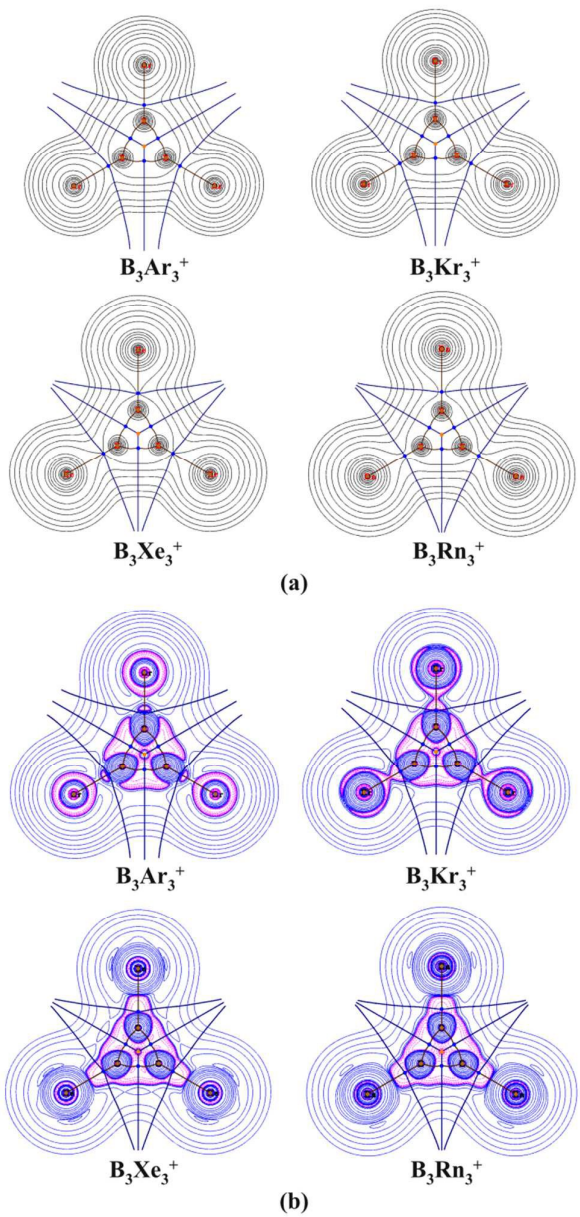


**Fig. 6.** Contour plots of (a) electron density and (b) Laplacian of the electron density ($\nabla^2\rho(\mathbf{r})$) of $B_3Ng_3^+$ (Ng = Ar – Rn) complexes at the MP2/def2-TZVP/WTBS level. (Black solid lines in (a) shows $\rho(\mathbf{r})$ contours; blue solid lines and magenta dashed lines in (b) show the region with $\nabla^2\rho(\mathbf{r}) > 0$ and region with $\nabla^2\rho(\mathbf{r}) < 0$ respectively)

**Energy Decomposition Analysis**

The EDA calculations of the $B_3Ng_3^+$ systems are carried out taking $B_3Ng_2^+$ as one fragment and one Ng atom as other (see Table 6). The positive and negative sign in the energy terms stand for the repulsive and attractive nature of the energies respectively. The maximum contribution towards the Ng–B bond stabilization comes from the $\Delta E^{orb}$, which ranges from 63.0-64.4% followed by $\Delta E^{elstat}$ (34.4-35.4%). The $\Delta E^{disp}$ (1.2-1.8%) contributes the lowest towards the total stabilization. The plots of deformation density are given in Fig. 7 and 2-SI. Here, the red colour stands for $\Delta\rho(\mathbf{r}) < 0$ and blue one is for $\Delta\rho(\mathbf{r}) > 0$, i.e., the electron density flows from red to blue region. The Ng $\rightarrow$ $B_3Ng_2^+$ σ-donation is found to be the major contribution towards the $\Delta E^{orb}$ for all Ng atoms. In the Ng $\rightarrow$ $B_3Ng_2^+$ σ-donation the shift in electron density, $\Delta\rho(\sigma_1)$ occurs from Ng atom which accumulates in between Ng and B centre that further gets shifted towards $B_3^+$ ring. Detailed molecular orbital consideration of the Ng and $B_3Ng_2^+$ fragments, highlights that the electron density shifts from the HOMO of Ng (choosing $p_z$ orbital) to the LUMO of the $B_3Ng_2^+$ (see Fig. 8) . The energy corresponding to this Ng $\rightarrow$ $B_3Ng_2^+$ σ-donation is abbreviated as $\Delta E^{\sigma1}$, which ranges from 72.9-78.1% of $\Delta E^{orb}$ for Ar-Rn analogues. $\Delta E^{\sigma1}$ gradually increases from Ar to Rn as similar to the $D_0$. The shortening of the B-B bond upon complexation with Ng can also be explained from the shape of $\Delta\rho(\sigma_1)$. Here the σ-donation clearly shows the accommodation of electron density in between the B-B bond of the $B_3^+$ ring. This accumulated electron density acts as an extra glue for the B-B bond which shortens the B-B bond. The next pair-wise orbital interaction comes from $B_3Ng_2^+$ $\rightarrow$ Ng back donation in which two orbital terms are originated from the $B_3Ng_2^+$ $\rightarrow$ Ng π-back donation($\Delta\rho(\pi_1)$, $\Delta E^{\pi1}$; $\Delta\rho(\pi_2)$, $\Delta E^{\pi2}$)) and one is $B_3Ng_2^+$ $\rightarrow$ Ng σ-back donation ($\Delta\rho(\sigma_2)$, $\Delta E^{\sigma2}$) (see Table 7 and Fig. 7). The $\Delta\rho(\pi_1)$ and $\Delta\rho(\pi_2)$ correspond to shifting of electron density from the HOMO of $B_3Ng_2^+$ to a vacant d orbital of Ng and HOMO-1 to another vacant d orbital of Ng, respectively. On the other hand, the electron density shift from HOMO-2 on $B_3Ng_2^+$ towards a vacant p orbital on Ng which is responsible for $B_3Ng_2^+$ $\rightarrow$ Ng σ-back donation.

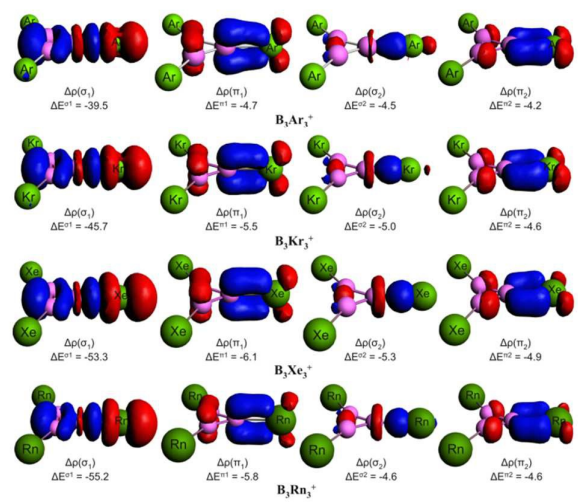


**Fig. 7.** Plots of deformation densities, $\Delta\rho(\mathbf{r})$, of the pair-wise orbital interactions in of $B_3Ng_3^+$ (Ng = Ar – Rn) complexes at the revPBE-D3/TZ2P//MP2/def2-TZVP level. The associated orbital interaction energies are given in kcal/mol. The colour code of the charge flow is red $\rightarrow$ blue.

**Table 7.** EDA results of the $B_3Ng_3^+$ (Ng = Ar – Rn) complexes considering Ng as one fragment and $B_3Ng_2^+$ as another fragment at the revPBE-D3/TZ2P//MP2/def2-TZVP level. All energy terms are in kcal/mol.

| Complex | $\Delta E^{Pauli}$ | $\Delta E^{elstat}$ | $\Delta E^{orb}$ | $\Delta E^{disp}$ | $\Delta E^{int}$ | $\Delta E^{\sigma 1}$ | $\Delta E^{\pi 1}$ | $\Delta E^{\sigma 2}$ | $\Delta E^{\pi 2}$ | $\Delta E^{rest}$ |
|---|---|---|---|---|---|---|---|---|---|---|
| $B_3Ar_3^+$ | 74.9 | -29.0 (34.4) | -54.2 (64.4) | -1.1 (1.2) | -9.4 | -39.5 (72.9) | -4.7 (8.7) | -4.5 (8.9) | -4.2 (7.7) | -0.9 |
| $B_3Kr_3^+$ | 84.9 | -34.4 (35.2) | -62.0 (63.5) | -1.3 (1.4) | -12.8 | -45.7 (73.7) | -5.5 (8.8) | -5.0 (8.1) | -4.6 (7.4) | -1.2 |
| $B_3Xe_3^+$ | 93.2 | -38.3 (34.6) | -70.7 (63.9) | -1.7 (1.5) | -17.6 | -53.3 (75.3) | -6.1 (8.7) | -5.3 (7.5) | -4.9 (6.9) | -1.1 |
| $B_3Rn_3^+$ | 93.2 | -39.5 (35.2) | -70.7 (63.0) | -2.0 (1.8) | -19.1 | -55.2 (78.1) | -5.8 (8.1) | -4.6 (6.5) | -4.6 (6.5) | -0.6 |

(The percentage values within the parentheses show the contribution towards the total attractive interaction $\Delta E^{elstat} + \Delta E^{orb} + \Delta E^{disp}$).

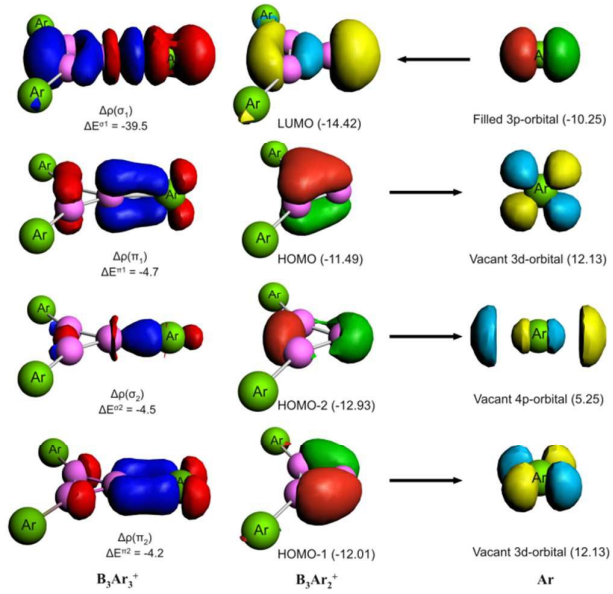


**Fig. 8.** Plots of the deformation densities, Δρ(**r**), and shape of the most important interacting orbitals of the pairwise orbital interactions between $B_3Ar_2^+$ and Ar in $B_3Ar_3^+$. The associated orbital interaction energies are given in kcal/mol. The colour code of the charge flow is red → blue.

## Conclusion

$B_3^+$ cluster shows a high tendency towards complexation with Ar-Rn atoms having each Ng-B bond dissociation energy in the range of 13.2-29.8 kcal/mol with gradual increase along Ar to Rn. The corresponding changes in enthalpy and free energy values for the dissociation processes highlight the thermochemical stability of $B_3Ng_3^+$ complexes. Localized Ng-B natural bond orbitals are noted in between Ng and B centres and consequently high Wiberg bond indices (0.57-0.78) are also found for Ng-B bonds, indicating these covalent natures of the bonds. Further, the electron density analysis also supports the covalent nature of the bonds where the local electron density is negative for all Ng-B bonds (Ng = Ar-Rn) and the Laplacian of electron density ($\nabla^2\rho(r_c)$) is negative for Xe/Rn-B bonds. Nevertheless, there is always an accumulation of electron density in between Ng and B centres as noted from the contour plots of $\nabla^2\rho(r_c)$. The energy decomposition analysis shows that the Ng-B bonds are mainly stabilized by of the orbital interaction energy (*ca.* 63.0-64.4%) and the electrostatic interaction energy (*ca.* 34.4-35.4%). Furthermore, the decomposition of orbital term into σ- and π-contributions reveals that the Ng-B bonding can be represented by a donor-acceptor model where the Ng (HOMO) → $B_3Ng_2^+$ (LUMO) σ-donation is a major contributor (*ca.* 72.9-78.1%) of the orbital term for Ar-Rn analogues. The σ- and π-back donations also occur from the occupied MOs of $B_3Ng_2^+$ to unoccupied MOs of Ng.

## Acknowledgements

PKC would like to thank DST, New Delhi for the J. C. Bose National Fellowship. RS and SM thank UGC, New Delhi for their fellowships. The work in México was supported by Conacyt (Grant CB-2015-252356). MO thanks Conacyt for his master fellowship.

## References

1 a) H. C. Brown, *J. Org. Chem.*, 1981, **46**, 4599; b) R. Kinjo, B. Donnadieu, M. A. Celik, G. Frenking and G. Bertrand, *Science*, 2011, **333**, 610; c) Y. Segawa, M. Yamashita and K. Nozaki, *Science*, 2006, **314**, 113; d) N. Miyaura and A. Suzuki, *Chem. Rev.*, 1995, **95**, 2457; e) T. Wideman and L. G. Sneddon, *Inorg. Chem.*, 1995, **34**, 1002; f) A. N. Alexandrova, A. I. Boldyrev, H.-J. Zhai and L.-S. Wang, *Coord. Chem. Rev.*, 2006, **250**, 2811.

2 a) D. Y. Zubarev, Analysis of Chemical Bonding in Clusters by Means of the Adaptive Natural Density Partitioning. All Graduate Theses and Dissertations, Paper 13, http://digitalcommons.usu.edu/etd/13, **2008**; b) M. Kimura, S. Suzuki, N. Shimakura, J. P. Gu, G. Hirsch, R. J. Buenker and I. Shimamura *Phys. Rev. A*, 1996, **54**, 3029; c) Y. S. Tergiman, F. Fraija and M. C. Bacchus-Montabonel, *Int. J. Quant. Chem.* 2002, **89**, 322; d) H.-J. Zhai, L.-S. Wang, A. N. Alexandrova, A. I. Boldyrev and V. G. Zakrzewski, *J. Phys. Chem. A*, 2003, **107**, 9319; e) T. R. Galeev, C. Romanescu, W.-L. Li, L.-S. Wang and A. I. Boldyrev, *J. Chem. Phys.*, 2011, **135**, 104301; f) A. P. Sergeeva1, B. B. Averkiev, H.-J. Zhai, A. I. Boldyrev and L.-S. Wang, *J. Chem. Phys.*, 2011, **134**, 224304; g) W. Huang, A. P. Sergeeva, H.-J. Zhai, B. B. Averkiev, L.-S. Wang and A. I. Boldyrev, *Nat. Chem.*, 2010, **2**, 202; h) I. A. Popov, V. F. Popov, K. V. Bozhenko, I. Černušák and A. I. Boldyrev, *J. Chem. Phys.*, 2013, **139**, 114307; i) T. Heine and G. Merino, *Angew. Chem. Int. Ed.*, 2012, **51**, 4275; j) G. Merino and T. Heine, *Angew. Chem. Int. Ed.*, 2012, **51**, 10226; k) J. M. Mercero, A. I. Boldyrev, G. Merino and J. M. Ugalde, *Chem. Soc. Rev.*, 2015, **44**, 6519; l) A. C. Castro, E. Osorio, J. L. Cabellos, E. Cerpa, E. Matito, M. Sola, M. Swart and G. Merino, *Chem. Eur. J.*, 2014, **16**, 4583; m) L. Liu, D. Moreno, E. Osorio, A. C. Castro, S. Pan, P. K. Chattaraj, T. Heine and G. Merino, *RSC Adv.*, 2016, **6**, 27177; n) G. Martínez-Guajardo, J. L. Cabellos, A. Díaz-Celaya, S. Pan, R. Islas, P. K. Chattaraj, T. Heine and G. Merino, *Sci. Rep.*, 2015, **5**, 11287; o) D. Moreno, S. Pan, G. Martínez-Guajardo, L. Lei-Zeonjuk, R. Islas, E. Osorio, P. K. Chattaraj, T. Heine and G. Merino, G. *Chem. Commun.*, 2014, **50**, 8140.

3 a) D. Martin, Y. Canac,. V. Lavallo and G. Bertrand *J. Am. Chem. Soc.*, 2014, **136**, 5023; b) H. Braunschweig, C.-W. Chiu, T. Kupfer and K. Radacki, *Inorg. Chem.*, 2011, **50**, 4247.

4 a) G. Frenking, *Nature*, 2015, **552**, 297; b) H. Braunschweig, R. D. Dewhurst, F. Hupp, M. Nutz, K. Radacki., C. W. Tate, A. Vargas and Q. Ye, *Nature*, 2015, **522**, 327.

5 a) H. Braunschweig, R. D. Dewhurst, K. Hammond, J. Mies, K. Radacki and A. Vargas *Science*, 2012, **336**, 1420; b) J. Böhnke, H. Braunschweig, P. Constantinidis, T. Dellermann, W. C. Ewing, I. Fischer, K. Hammond, F. Hupp, J. Mies, H.-C. Schmitt and A. Vargas, *J. Am. Chem. Soc.*, 2015, **137**, 1766; c) H. Braunschweig, T. Dellermann, R. D. Dewhurst, W. C. Ewing, K. Hammond, J. O. C. Jimenez-Halla, T. Kramer, I. Krummenacher, J. Mies, A. K. Phukan and A. Vargas, *Nat. Chem.*, 2013, 5, 1025; d) M. Zhou, N. Tsumori, Z. Li, K. Fan, L. Andrews and Q. Xu, *J. Am. Chem. Soc.*, 2002, **126**, 12936; e) S.-D. Li, H.-J. Zhai and L.-S. Wang, *J. Am. Chem. Soc.*, 2008, **130**, 2573.

6 a) T. B. Tai, N. M. Tam and M. T. Nguyen, *Theor. Chem. Acc.*, 2012, **131**, 1241; b) D. Y. Zubarev and A. I. Boldyrev, *J. Comput. Chem.*, 2007, **28**, 251.

7 T. B. Tai and M. T. Nguyen, *Angew. Chem. Int. Ed.,* 2013, **52**, 4554.

8 a) X.-W. Li, W. T. Pennington and G. H. Robinson, *J. Am. Chem. Soc.*, 1995, **117**, 7578; b) X.-W. Li, Y. Xie, P. Schreiner, K.D. Gripper, R. C. Crittendon, C. Campana, H. F. Schaefer and G. H. Robinson, *Organometallics*, 1996, **15**, 3798.

9 R. J. Wright, M. Brynda and P. P. Power, *Angew. Chem. Int. Ed.,* 2006, **45**, 5953.

10 J. Jin, G. Wang, M. Zhou, D. M. Andrada, M. Hermann and G. Frenking, *Angew. Chem. Int. Ed.*, 2016, **55**, 2078.

11 a) N. Bartlett, *Proc. Chem. Soc.*, 1962, 218; b) L. Graham, O. Graudejus, N. K. Jha and N. Bartlett, *Coord. Chem. Rev.*, 2000, **197**, 321.

12 R. Hoppe, W. Daehne, H. Mattauch and K. Roedder, *Angew. Chem., Int. Ed. Engl*. 1962, **1**, 599.

13 H. H. Claassen, H. Selig and J. G. Malm, *J. Am. Chem. Soc.*, 1962, **84**, 3593.

14 P. R. Fields, L. Stein and M. H. Zirin, *J. Am. Chem. Soc.*, 1962, **84**, 4164.

15 J. J. Turner and G. C. Pinetel, *Science*, 1963, **140**, 974.

16 a) C. A. Thompson and L. Andrews, *J. Am. Chem. Soc.*, 1994, **116**, 423; b) J. Li, B. E. Bursten, B. Liang and L. Andrews, *Science*, 2002, **295**, 2242. c) B. Liang, L. Andrews, J. Li and B. E. Bursten, *J. Am. Chem. Soc.*, 2002, **124**, 9016; d) X. Wang, L. Andrews, J. Li and B. E. Bursten, *Angew. Chem. Int. Ed.*, 2004, **43**, 2554. e) V. I. Feldman, F. F. Sukhov and A. Y. Orlov, *Chem. Phys. Lett.*, 1997, **280**, 507; f) L.Khriachtchev, H. Tanskanen, M. Pettersson, M. Räsänen, J. Ahokas, H. Kunttu and V. Feldman, *J. Chem. Phys.*, 2002, **116**, 5649; g) V. I. Feldman, F. F. Sukhov, A. Yu. Orlov and I. V. Tyulpina, *J. Am. Chem. Soc.*, 2003, **125**, 4698; h) M. Pettersson, J. Lundell, L. Khriachtchev, L. Isamieni and M. Räsänen, *J. Am. Chem. Soc.*, 1998, **120**, 7979; i) M. Pettersson, J. Lundell, L. Khriachtchev and M. Räsänen, *J. Chem. Phys.*, 1998, **109**, 618; j) M. Pettersson, L. Khriachtchev, J. Lundell and M. Räsänen, *J. Am. Chem. Soc.*, 1999, **121**, 11904; k) L. Khriachtchev, M. Pettersson, N. Runeberg, J. Lundell and M. Räsänen, *Nature*, 2000, **406**, 874; l) L. Khriachtchev, M. Pettersson, A. Lignell and M. Räsänen, *J. Am. Chem. Soc.*, 2001, **123**, 8610; m) L. Khriachtchev, M. Pettersson, J. Lundell, H. Tanskanen, T. Kiviniemi, N. Runeberg and M. Räsänen, *J. Am. Chem. Soc.*, 2003, **125**, 1454; n) S. A. Cooke and M. C. L. Gerry, *J. Am. Chem. Soc.*, 2004, **126**, 17000; o) J. M. Michaud, S. A. Cooke and M. C. L. Gerry, *Inorg. Chem.*, 2004, **43**, 3871; p) J. M. Thomas, N. R. Walker, S. A. Cooke and M. C. L. Gerry, *J. Am. Chem. Soc.*, 2004, **126**, 1235; q) S. A. Cooke and M. C. L. Gerry, *Phys. Chem. Chem. Phys.*, 2004, **6**, 3248; r) S. A. Cooke and M. C. L. Gerry, *J. Am. Chem. Soc.*, 2004, **126**, 17000; s) J. M. Michaud and M. C. L. Gerry, *J. Am. Chem*. Soc., 2006, **128**, 7613; t) D. S. Brock, H. P. A. Mercier and G. J. Schrobilgen, *J. Am. Chem. Soc.*, 2013, **135**, 5089; u) G. L. Smith, H. P. A. Mercier and G. J. Schrobilgen, *Inorg. Chem.*, 2011, **49**, 12359; v) J. R. Debackere, H. P. A. Mercier and G. J. Schrobilgen, *J. Am. Chem. Soc.,* 2014, **136**, 3888.

17 a) W. Koch, B. Liu and G. Frenking, *J. Chem. Phys.*, 1990, **92**, 2464; b) G. Frenking, W. Koch, F. Reichel and D. Cremer, *J. Am. Chem. Soc.*, **1990**, *112*, 4240; c) S. Pan, A. Gupta, S. Mandal, D. Moreno, G. Merino and P. K. Chattaraj, *Phys. Chem. Chem. Phys.*, 2015, **17**, 972; d) R. Saha, S. Pan, G. Merino and P. K. Chattaraj, *J. Phys. Chem. A*, 2015, **119**, 6746; e) J. Lundell, A. Cohen and R. B. Gerber, *J. Phys. Chem. A*, 2002, **106**, 11950; f) W. A. Grochala, *Phys. Chem. Chem. Phys.*, 2012, **14**, 14860; g) G. Frenking, W. Koch, D. Cremer, J. Gauss and J. F. Liebman, *J. Phys. Chem.* 1988, **93**, 3410; h) S. Pan, D. Moreno, J. L. Cabellos, J. Romero, A. Reyes, G. Merino and P. K. Chattaraj, *J. Phys. Chem. A*, 2014, **118**, 487; i) L. Khriachtchev, M. Räsänen and R. B. Gerber, *Acc. Chem. Res.* 2009, **42**, 183; j) G. Frenking, W. J. Gauss and D. Cremer, *J. Am. Chem. Soc.*, 1988, **110**, 8007; k) G. Leroy and M. Sana, *Theor. Chim. Acta.*, 1990, **77**, 383; l) S. Pan, M. Contreras, J. Romero, A. Reyes, G. Merino and P. K. Chattaraj, *Chem. Eur. J.*, 2013, **19**, 2322; m) S. Pan, R. Saha, S. Mandal and P. K. Chattaraj, *Phys. Chem. Chem. Phys.* 2016, **18**, 11661; n) L. Operti, R. Rabezzana, F. Turco, S. Borocci, M. Giordani and F. Grandinetti, *Chem. Eur. J.* 2011, **17**, 10682; o) S. Borocci , M. Giordani and F. Grandinetti, *J. Phys. Chem. A* 2015, **119**, 2383; p) S. Pan, A. Gupta, R. Saha, G. Merino and P. K. Chattaraj, *J. Comp. Chem.* 2015, **36**, 2168; q) S. Pan, D. Moreno, S. Ghosh, G. Merino and P. K. Chattaraj, *J. Comp. Chem.,* 2016, **37**, 226; r) S. Pan, S. Jalife, M. Kumar, V. Subramanian, G. Merino, and P. K. Chattaraj, *ChemPhysChem,* 2013, **14**, 2511; s) S. Pan, S. Jalife, R. M. Kumar, V. Subramanian, G. Merino and P. K. Chattaraj, *ChemPhysChem,* 2013, **14**, 2511; t) S. Pan, R. Saha, and P. K. Chattaraj, *New J. Chem.* 2015, **39**, 6778; u) P. Szarek and W. Grochala, *J. Phys. Chem. A,* 2015, **119**, 2483; v) Q. Zhang, M. Chen, M. Zhou, D. M. Andrada and G. Frenking, *J. Phys. Chem. A,* 2015, **119**, 2543; w) S. Pan, R. Saha, A. Kumar, A. Gupta, G. Merino and P. K. Chattaraj, *Int. J. Quantum Chem.*, 2016, **116**, 1016.

18 a) C. Zhu, K. Niimi, T. Taketsugu, M. Tsuge, A. Nakayama and L. Khriachtchev, *J. Chem. Phys.*, 2015, **142**, 054305; b) C. Cheng and L. Sheng, *Comp. Theor. Chem.,* 2012, **989**, 39; c) J. Ahokas, K. Vaskonen, J. Eloranta and H. Kunttu, *J. Phys. Chem. A* 2000, **104**, 9506; d) P. Antoniotti, S. Borocci, N. Bronzolino, P. Cecchi and F. Grandinetti, *J. Phys. Chem. A*, 2007, **111**, 10144; e) J.-L. Chen , C.-Y. Yang , H.-J. Lin and W.-P. Hu, *Phys. Chem. Chem. Phys.*, 2013, **15**, 9701; f) T.-Y. Lin, J.-B. Hsu, W.-P. Hu, *Chem. Phys. Lett.*, 2005, **402**, 514; g) A. Ghosh, S. Dey, D. Manna, and T. K. Ghanty, *J. Phys. Chem. A*, 2015, **119**, 5732; h) T. Jayasekharan and T. K. Ghanty, *J. Chem. Phys.*, 2008, **129**, 184302; i) A. Ghosh, D. Manna and T. K. Ghanty, *J. Phys. Chem. A* 2015, **119**, 2233; j) P. Sekhar, A. Ghosh and T. K. Ghanty, *J. Phys. Chem. A*, 2015, **119**, 11601; k) L. Khriachtchev, H. Tanskanen, J. Lundell, M. Pettersson, H. Kiljunen, and Markku

Räsänen, *J. Am. Chem. Soc.*, 2003, **125**, 4696; l) C. T. Goetschel and K. R. Loos, *J. Am. Chem. Soc.*, 1972, **94** , 3018 m) Joel F. Liebman, Leland C. Allen, *Inorg. Chem.*, 1972, **11**, 114; n) J. T. Koskinen and R. Graham Cooks, *J. Phys. Chem. A*, 1999, **103**, 9567; o) A. Papakondylis, E. Miliordos and A. Mavridis, *J. Phys. Chem. A*, 2004, **108**, 4335.

19 a) C. Møller and M. S. Plesset, *Phys. Rev.*, 1934, **46**, 618; b) M. Head-Gordon and J. A. Pople, *Chem. Phys. Lett*., 1988, **153**, 503.

20 a) J. Čížek, *J. Chem. Phys.*, 1966, **45**, 4256; b) J. Čížek, *Adv. Chem. Phys*., 1969, **14**, 35; c) R. J. Bartlett and M. Musial, *Rev. Mod. Phys.*, 2007, **79**, 291.

21 a) F. Weigend and R. Ahlrichs, *Phys. Chem. Chem. Phys.*, 2005, **7**, 32975; b) A. Anoop, W. Thiel and F. Neese, *J. Chem. Theory Comput.*, 2010, **6**, 3137; c) Orca manual, Version 3.0, pp-56, https://orcaforum.cec.mpg.de/OrcaManual.pdf.

22 K. A. Peterson, D. Figgen, E. Goll, H. Stoll and M. Dolg, *J. Chem. Phys*., 2003, **119**, 11113.

23 S. F. Boys and F. Bernardi, *Mol. Phys.*, 1970, **19**, 553.

24 A. E. Reed, R. B. Weinstock and F. Weinhold, *J. Chem. Phys.* 1985, **83**, 735.

25 K. B. Wiberg, *Tetrahedron*., 1968, **24**, 1083.

26 A. E. Reed, L. A. Curtiss and F. Weinhold, *Chem. Rev.,* 1988, **88**, 899.

27 M. J. Frisch, *et al.* Gaussian 09, Revision C.01, Gaussian, Inc., Wallingford CT, 2009.

28 R. F. W. Bader, *Atoms in Molecules: A Quantum Theory*, Oxford University Press: Oxford, UK, **1990**.

29 T. Lu and F. W. Chen, *J. Comput. Chem*., 2012, **33***,* 580.

30 S. Huzinaga and M. Klobukowski, *Chem. Phys. Lett*., **1993**, *212*, 260-264.

31 M. P. Mitoraj, A. Michalak and T. A. Ziegler, *J. Chem. Theory Comput.*, 2009, **5**, 962.

32 a) E. J. Baerends, *et al. ADF2013.01*, SCM, *Theoretical Chemistry*, Vrije Universiteit, Amsterdam, The Netherlands, 2013 b) G. te Velde, F. M. Bickelhaupt, E. J. Baerends, C. F. Guerra, S. J. A. Van Gisbergen, J. G. Snijders and T. Ziegler, *J. Comput. Chem.*, 2001, **22**, 931.

33 L. Goerigk and S. Grimme, *Phys. Chem. Chem. Phys*., 2011, **13**, 6670.

34 E. van Lenthe, A. Ehlers and E.-J. Baerends, *J. Chem. Phys.*, 1999, **110**, 8943.

35 G. F. Caramori, R. M. Piccoli, M. Segal, A. Muñoz-Castro, R. Guajardo-Maturana, D. M. Andradae and G. Frenking, *Dalton Trans.*, 2015, **44**, 377.

36 B. Cordero, V. Gómez, A. E. Platero-Prats, M. Revés, J. Echeverría, E. Cremades, F. Barragán and S. Alvarez, *Dalton Trans*., **2008**, 2832–2838.

37 a) P. Macchi, D.M. Proserpio and A. Sironi, *J. Am. Chem. Soc.*, 1998, **120**, 13429; b) P. Macchi, L. S. Garlaschelli, S. Martinengo and A. Sironi, *J. Am. Chem. Soc.*, 1999, **121**, 10428; c) I. V. Novozhilova, A. V. Volkov and P. Coppens, *J. Am. Chem. Soc.*, 2003, **125**, 1079; d) D. Cremer and E. Kraka, *Angew. Chem. Int. Ed*., 1984, **23**, 627.

## Graphical Abstract

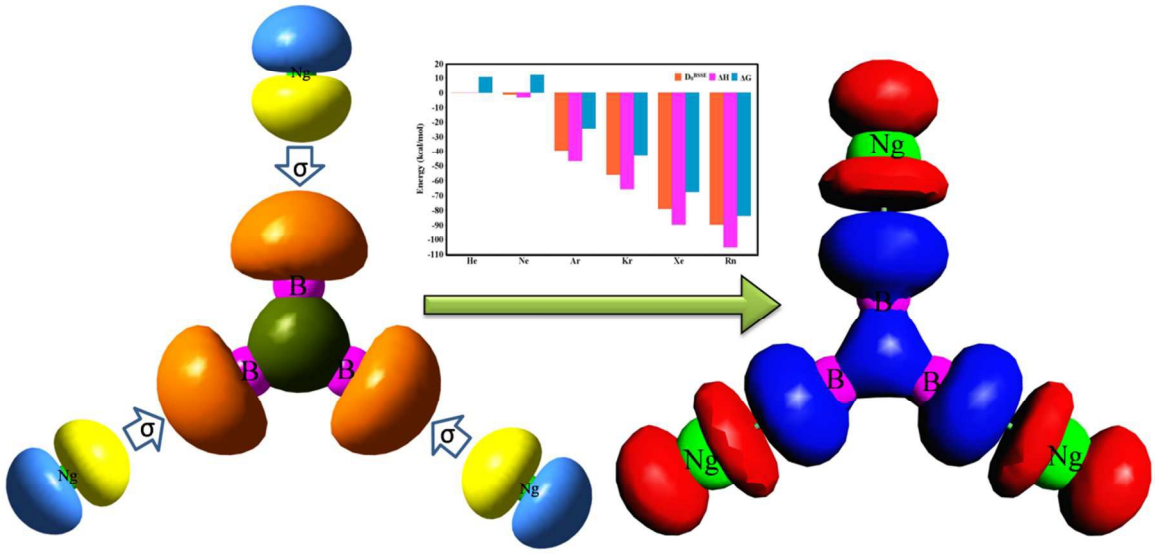


Ar to Rn atoms formed exceptionally strong bonds with $B_3^+$ where the Ng (HOMO) → $B_3Ng_2^+$ (LUMO) σ-donation is the key term to stabilize the complexes.